# A Monte Carlo approach to the joint estimation of reservoir and elastic parameters from seismic amplitudes

Miguel Bosch<sup>1</sup>, Luis Cara<sup>1</sup>, Juan Rodrigues<sup>1</sup>, Alonso Navarro<sup>2</sup>, and Manuel Díaz<sup>2</sup>

#### **ABSTRACT**

Inversion of seismic data and quantification of reservoir properties, such as porosity, lithology, or fluid saturation, are commonly executed in two consecutive steps: a geophysical inversion to estimate the elastic parameters and a petrophysical inversion to estimate the reservoir properties. We combine within an integrated formulation the geophysical and petrophysical components of the problem to estimate the elastic and reservoir properties jointly. We solve the inverse problem following a Monte Carlo sampling approach, which allows us to quantify the uncertainties of the reservoir estimates accounting for the combination of geophysical data uncertainties, the deviations of the elastic properties from the calibrated petrophysical transform, and the nonlinearity of the geophysical and petrophysical relations. We implement this method for the inference of the total porosity and the acoustic impedance in a reservoir area, combining petrophysical and seismic information. In our formulation, the porosity and impedance are related with a statistical model based on the Wyllie transform calibrated to well-log data. We simulate the seismic data using a convolutional model and evaluate the geophysical likelihood of the joint porosity-impedance models. Applying the Monte Carlo sampling method, we generate a large number of realizations that jointly explain the seismic observations and honor the petrophysical information. This approach allows the calculation of marginal probabilities of the model parameters, including medium porosity, impedance, and seismic source wavelet. We show a synthetic validation of the technique and apply the method to data from an eastern Venezuelan hydrocarbon reservoir, satisfactorily predicting the medium stratification and adequate correlation between the seismic inversion and well-log estimates for total porosity and acoustic impedance.

### INTRODUCTION

Methods for inferring reservoir parameters, such as porosity, shale volume, and fluid volume fractions, are based on two major steps of estimation: the seismic and the petrophysical inversion. In the former, knowledge about seismic wave propagation is used to obtain a description of the elastic properties in the reservoir, or seismic attributes, from the seismic data. In the latter, petrophysical information obtained from, or calibrated to, well-log data is used to estimate the reservoir parameters from the seismically derived parameters

Current techniques separate these two inversion steps following different methods. Elastic parameters are estimated from partially stacked seismic sections (e.g., Mukerji et al., 2001; Contreras et al., 2005) and then related to discrete facies and fluids with a statistical model built from the well-log data. Prestacked data are used to estimate amplitude-variation-with-offset (AVO) parameters (e.g., Eidsvik et al., 2004), which are used in turn to estimate discrete facies and fluids using a statistical model based on well-log data. Reservoir parameters are estimated using a spatial statistical model conditioned by elastic parameters and well-log data (Doyen, 1988; Contreras et al., 2005) or using Monte Carlo simulations conditioned by elastic parameters (Bachrach, 2006). In all of these works, reservoir-parameter estimation is based on the previous seismic inversion step.

Concerning the petrophysical models used to relate reservoir and seismically derived properties, different approaches have been followed. Deterministic models, based on either theoretical or empirical information, describe in an exact way the relation between reservoir and elastic parameters. These models, such as those of Wyllie, Gassman, and Archie, summarize fundamental behavior of the rock properties, although the actual core or well-log data do not match the model prediction exactly. Conversely, purely statistical models describe probabilities for the reservoir parameters conditioned by the seismic-derived properties, or vice-versa, on the basis of the empirical statistical characterization of the well-log data of the area. This is the approach followed in the research of Doyen (1988), Mukerji et

Manuscript received by the Editor 13 February 2007; revised manuscript received 7 June 2007; published online 10 October 2007.

<sup>1</sup>Central University of Venezuela, Geophysical Simulation and Inversion Laboratory, Engineering Faculty, Caracas, Venezuela. E-mail: boschm@ucv.ve; luiscara1@yahoo.es; jmiguelrt@cantv.net.

<sup>2</sup>Petrobaras Energía Venezuela, Caracas, Venezuela. E-mail: alonso.navarro@petrobras.com; manuel.diaz@petrobras.com. © 2007 Society of Exploration Geophysicists. All rights reserved.

O30 Bosch et al.

al. (2001), Eidsvik et al. (2004), Larsen et al. (2006), and Contreras et al. (2005). These models describe data variability, but they are very dependent on the spatial heterogeneity of the statistics and the size of the data set on which they are based. Finally, mixed models, which include basic petrophysical functions and describe the data deviation from the function as a random variable that follow a statistical model, are robust in honoring rock behavior and accurate in describing the parameters' variability. This approach is followed in work by Bosch (2004), Bachrach (2006), and Loures and Moraes (2006), and it is followed here as well.

A general strategy for combining the petrophysical and geophysical inversion steps under a unified statistical inference framework is proposed by Bosch (1999) and applied to the joint inversion of gravity and magnetic data to infer discrete lithology (Bosch et al., 2001; Bosch and McGaughey, 2001). In this formulation, the likelihoods with the geophysical observations and the petrophysical relations across modeled properties are honored jointly in realizations of the model obtained with a Monte Carlo method. The formulation has been further developed to account for the estimation of continuous properties, such as porosity, with application to reservoir description (Bosch, 2004). In the latter work, a set of linearized equations is used to update porosity and acoustic impedance jointly, fitting stacked seismic data and petrophysical relations within uncertainties and showing that the integrated inversion produces a better estimate than a stepwise procedure, particularly if the petrophysical transform is nonlinear.

The development of methods for combining the geophysical and petrophysical inference steps involved in reservoir description is a major motivation of the current work. An advantage of this approach is that the petrophysical and geophysical information is combined, increasing constraints on the model parameters and reducing uncertainty in the estimates. In addition, an integrated formulation allows adequate quantification of the uncertainty associated with combining the different components of the information. Using an integrated statistical formulation, we develop a Monte Carlo sampling approach to explore the model space, providing joint estimation of the reservoir and the elastic parameters and detailed description of their probability, i.e., full description of the parameter uncertainties.

The relation between the elastic and reservoir parameters follows a mixed model, based on a petrophysical relation and a statistical description of the deviations from the relation. We employ Markov Chain Monte Carlo techniques to generate a large number of model realizations that jointly honor the petrophysical and geophysical likelihoods and prior geostatistical information about the porosity.

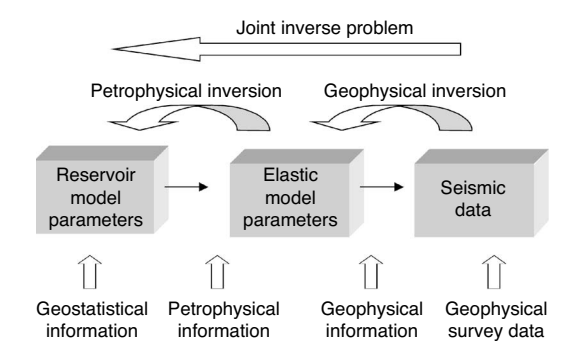


Figure 1. Types of information, model parameters, and data spaces included in the inference problem. Black arrows indicate the sense of the forward problem.

The method is applied to data from an eastern Venezuelan hydrocarbon reservoir to obtain estimates and marginal probabilities of porosity and acoustic impedance. A preliminary description of this approach is shown by Bosch and Fernández (2003) and Bosch et al. (2006).

Other methods to integrate the petrophysical and geophysical inversion steps for reservoir characterization have focused on predicting discrete lithology, as in the work by Torres-Verdin et al. (1999) using a simulated annealing technique and in the work of Gonzalez et al. (2006) based on Monte Carlo sampling techniques. Larsen et al. (2006) propose a method of integrated inversion to infer discrete lithology from seismic amplitude-variation-with-angle (AVA) data and show a synthetic 1D example.

#### THEORY AND METHOD

We consider a joint model space, describing reservoir and elastic medium property fields, and a data space, describing seismic survey observations. Figure 1 is a schematic of the model parameter and data spaces. The joint model space can be regarded as the product of the two subspaces, corresponding to the description of the geologically and physically related properties. Each of the subspaces could be composed of several property fields.

To relate these subspaces and the data space, we introduce three types of information into the inference problem: geostatistical, petrophysical, and geophysical. The first type refers to the geostatistical description of the reservoir fields, the second defines the relation between reservoir and elastic parameter fields based on a statistical and petrophysical model, and the third is associated with the relation between the elastic fields and the observations of the seismic survey (i.e., our forward simulation method that calculates seismic data from the elastic field and the model likelihood with the observations).

## Statistical formulation

We denote with  $\mathbf{m}_{\text{geo}}$  a set of parameters that defines the reservoir-property fields and with  $\mathbf{m}_{\text{phys}}$  the set of parameters that defines the elastic-property fields. Table 1 shows a list of symbols used in this work. Following a Bayesian approach, we describe the knowledge of the porosity and impedance profiles with a statistical model in the parameter space. Given a joint model configuration  $\mathbf{m} = (\mathbf{m}_{\text{geo}}, \mathbf{m}_{\text{phys}})$ , we define a probability density that combines the available information and data. We start from the common equation for statistical inference (Tarantola, 2005),

$$\sigma(\mathbf{m}) = cL(\mathbf{m})\rho(\mathbf{m}),\tag{1}$$

where  $\rho(\mathbf{m})$  is the prior information probability density,  $L(\mathbf{m})$  is the data likelihood function, c is a normalization constant, and  $\sigma(\mathbf{m})$  is the posterior probability density. We decompose the prior density and the likelihood function in terms of the model subspaces already defined,

$$\sigma(\mathbf{m}_{\text{phys}}, \mathbf{m}_{\text{geo}}) = cL(\underbrace{\mathbf{m}_{\text{phys}}}) \pi(\underbrace{\mathbf{m}_{\text{phys}}|\mathbf{m}_{\text{geo}}}) \rho_{\underbrace{\text{geo}}} (\mathbf{m}_{\text{geo}}).$$
(2)

The combined probability density is given by the product of three factors, each one summarizing one of the types of information included in our problem. The probability density function (PDF)  $\rho_{\rm geo}(\mathbf{m}_{\rm geo})$  describes the prior information in the reservoir property fields. The conditional probability density  $\pi(\mathbf{m}_{\rm phys}|\mathbf{m}_{\rm geo})$  is a petrophysical likelihood function. It measures the probability of the elastic property fields given a particular reservoir field configuration. The factor  $L(\mathbf{m}_{\rm phys})$  is the geophysical likelihood function that mea-

sures the proximity between the observed and calculated seismic data. It depends on the elastic property field parameters. More information about this formulation can be found in Bosch (1999) and Bosch et al. (2001).

The modeled seismic data are also dependent on the seismic source function, which is not measured directly. It is commonly estimated from well logs and seismic data. To take into account the uncertainty associated with estimating the source function, we include it as an additional random variable in the statistical model. Thus, we extend this formulation and compose the model parameters by  $\mathbf{m} = (\mathbf{m}_{\text{geo}}, \mathbf{m}_{\text{phys}}, \mathbf{m}_{\text{sou}})$ , where  $\mathbf{m}_{\text{sou}}$  is the parameter set describing the source wavelet. The joint geophysical likelihood function can be formulated by

$$L(\mathbf{m}_{\text{phys}}, \mathbf{m}_{\text{sou}}) = L(\mathbf{m}_{\text{phys}} | \mathbf{m}_{\text{sou}}) \rho_{\text{sou}}(\mathbf{m}_{\text{sou}}),$$
(3)

where the probability density  $\rho_{\text{sou}}(\mathbf{m}_{\text{sou}})$  describes the prior information about the seismic source function, and the seismic data likelihood,  $L(\mathbf{m}_{\text{phys}}|\mathbf{m}_{\text{sou}})$ , is conditioned by the source parameters.

The combined joint PDF, including the source function random parameters, is given by

$$\begin{split} &\sigma(\mathbf{m}_{\text{phys}}, \mathbf{m}_{\text{geo}}, \mathbf{m}_{\text{sou}}) \\ &= c L(\mathbf{m}_{\text{phys}} | \mathbf{m}_{\text{sou}}) \underbrace{\pi(\mathbf{m}_{\text{phys}} | \mathbf{m}_{\text{geo}})}_{\text{petrophysics}} \underbrace{\rho_{\text{geo}}(\mathbf{m}_{\text{geo}}) \rho_{\text{sou}}(\mathbf{m}_{\text{sou}})}_{\text{geostatistics}}. \end{split}$$

We model each of the factors of the combined PDF with multivariate parametric functions and set up a sampling algorithm to produce realizations of the combined density. The prior densities for the reservoir and source parameters are modeled as multivariate Gaussian functions of the parameters,

$$\rho_{\text{geo}}(\mathbf{m}_{\text{geo}}) = c_1 \exp \left[ -\frac{1}{2} (\mathbf{m}_{\text{geo}} - \mathbf{m}_{\text{geo prior}})^{\text{T}} \mathbf{C}_{\text{geo}}^{-1} \right] \times (\mathbf{m}_{\text{geo}} - \mathbf{m}_{\text{geo prior}}) ,$$
(5)

$$\rho_{\text{sou}}(\mathbf{m}_{\text{sou}}) = c_2 \exp \left[ -\frac{1}{2} (\mathbf{m}_{\text{sou}} - \mathbf{m}_{\text{sou prior}})^T \mathbf{C}_{\text{sou}}^{-1} \right] \times (\mathbf{m}_{\text{sou}} - \mathbf{m}_{\text{sou prior}}) ,$$
(6)

Table 1. List of basic symbols used to formulate the inverse problem.

Symbol	Description
$\mathbf{m}_{\mathrm{phys}}$	Elastic property model parameter array
$\mathbf{m}_{\mathrm{geo}}$	Reservoir property model parameter array
$\mathbf{m}_{\mathrm{sou}}$	Seismic source wavelet model parameter array
m	Joint model parameter array
$\mathbf{d}_{\mathrm{obs}}$	Observed seismic data
$\mathbf{d}_{\mathrm{calc}}$	Calculated seismic data
$\sigma(\mathbf{m}_{ ext{phys}},\mathbf{m}_{ ext{geo}},\mathbf{m}_{ ext{sou}})$	Joint posterior probability density
$ ho_{ m geo}({f m}_{ m geo})$	Prior probability density on the reservoir parameters
$ ho_{ m sou}({f m}_{ m sou})$	Prior probability density on the source wavelet
$\pi(\mathbf{m}_{ ext{phys}} \mathbf{m}_{ ext{geo}})$	Probability density of the elastic property parameters conditioned by the reservoir parameters
$L(\mathbf{m}_{phys}, \mathbf{m}_{sou})$	Joint seismic likelihood function
$L(\mathbf{m}_{ ext{phys}} \mathbf{m}_{ ext{sou}})$	Seismic likelihood function conditioned by a known source configuration
$\mathbf{m}_{ ext{geo prior}}$	Prior reservoir property model configuration
$\mathbf{m}_{ ext{sou prior}}$	Prior seismic source wavelet model configuration
$c, c_1, c_2$	Normalization constants
$\mathbf{g}(\mathbf{m}_{ ext{phys}})$	Function solving the geophysical forward problem
$\mathbf{f}(\mathbf{m}_{\mathrm{geo}})$	Function providing the mean model elastic parameters conditioned by the model reservoir parameters
$\mathbf{C}_{ ext{dat}}$	Data covariance matrix
$\mathbf{C}_{ ext{geo}}$	Prior covariance matrix for the reservoir model parameters
$\mathbf{C}_{ ext{sou}}$	Prior covariance matrix for the source model parameters
$\mathbf{C}_{ ext{phys}  ext{geo}}$	Prior covariance matrix for the elastic model parameters conditioned by the reservoir model parameters
$\phi$	Layer total porosity
$\boldsymbol{\phi}^*$	Layer logarithmic porosity
Z	Layer acoustic impedance
$V_{ m matrix}$	Rock matrix compressional velocity in Wyllie relation
$V_{ m fluid}$	Rock fluid compressional velocity in Wyllie relation
$ ho_{ ext{matrix}}$	Rock matrix mass density in Wyllie relation
$ ho_{ m fluid}$	Rock fluid mass density in Wyllie relation

O32 Bosch et al.

where  $\mathbf{m}_{\text{geo prior}}$  and  $\mathbf{m}_{\text{sou prior}}$  are the reservoir and source parameters expected from the prior information,  $\mathbf{C}_{\text{geo}}$  and  $\mathbf{C}_{\text{sou}}$  are the corresponding covariance matrices,  $c_1$  and  $c_2$  are normalization constants, and the superscript T indicates array transposition. The normalization constants are not needed for the implementation of the sampling algorithms.

The geophysical likelihood is defined as a Gaussian function of the deviations of the observed seismic data  $\mathbf{d}_{obs}$  and the seismic data calculated from the model configuration  $\mathbf{d}_{cal}$ . The latter depends on the function that simulates the seismic response of the model  $\mathbf{d}_{cal}$  =  $\mathbf{g}(\mathbf{m}_{phys}, \mathbf{m}_{sou})$ , commonly a nonlinear function. Thus, we model the geophysical likelihood as follows:

$$L(\mathbf{m}_{phys}|\mathbf{m}_{sou}) = \exp\left[-\frac{1}{2}(\mathbf{d}_{obs} - \mathbf{g}(\mathbf{m}_{phys}, \mathbf{m}_{sou}))^{T} \times \mathbf{C}_{dat}^{-1}(\mathbf{d}_{obs} - \mathbf{g}(\mathbf{m}_{phys}, \mathbf{m}_{sou}))\right], \quad (7)$$

with  $C_{\text{dat}}$  the data covariance matrix.

Similarly, the petrophysical likelihood function is modeled as a multivariate Gaussian function of deviations between the physical model parameters  $\mathbf{m}_{phys}$ , and their corresponding value is predicted by a petrophysical function of the reservoir parameters  $\mathbf{f}(\mathbf{m}_{geo})$ , commonly a nonlinear function:

$$\pi(\mathbf{m}_{\text{phys}}|\mathbf{m}_{\text{geo}}) = \exp\left[-\frac{1}{2}(\mathbf{m}_{\text{phys}} - \mathbf{f}(\mathbf{m}_{\text{geo}}))^{T}\mathbf{C}_{\text{phys}|\text{geo}}^{-1}\right] \times (\mathbf{m}_{\text{phys}} - \mathbf{f}(\mathbf{m}_{\text{geo}}))^{T}.$$
(8)

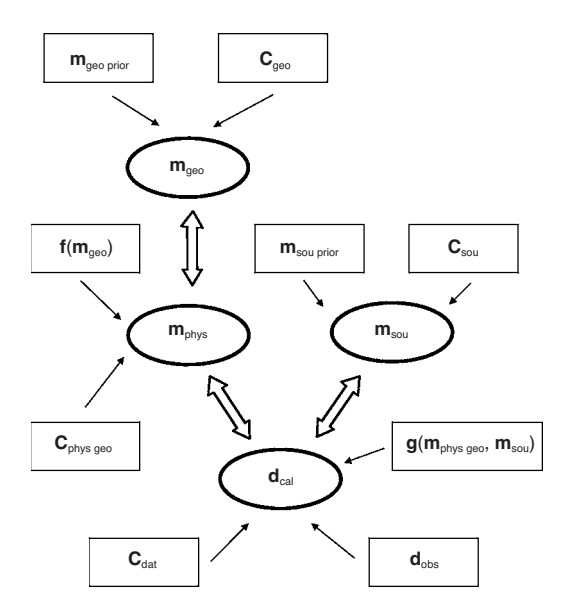


Figure 2. Parameters involved in the inference problem and their relations. Enclosed in ovals: random parameters defining medium properties, source function, and calculated seismic data. Enclosed in boxes: nonrandom parameters and functions defining the probability model for the random parameters and their relations. Arrows indicate dependencies with nonrandom parameters (thin arrows) and random parameters (thick arrows). Symbols are described in Table 1.

Modeling the four factors shown in equations 5–8 fully defines the combined probability in equation 4. The combined probability depends on the seismic observed data, functions  $\mathbf{f}(\mathbf{m}_{geo})$  and  $\mathbf{g}(\mathbf{m}_{phys},\mathbf{m}_{sou})$  solving the petrophysical and geophysical forward problems correspondingly, mean priors for the source wavelet and the reservoir fields, and covariance matrices for data misfit, petrophysical misfit, source, and reservoir prior densities. Figure 2 graphs the relations between model parameters, statistical parameters, and data

Note that the petrophysical and geophysical likelihoods have been defined with Gaussian functions of the deviations between model parameters and nonlinear functions  $\mathbf{f}(\mathbf{m}_{\text{geo}})$  and  $\mathbf{g}(\mathbf{m}_{\text{phys}},\mathbf{m}_{\text{sou}})$ . Thus, these likelihoods are not Gaussian functions of the model parameters; neither is the combined probability density a Gaussian function of the model parameters. Depending on the geophysical and petrophysical forward functions, the combined density may be a complicated, eventually multimodal probability density.

# Monte Carlo sampling

Two major approaches can be followed to solve the inference problem based on the combined probability density (equation 4): sampling or optimization. An optimization approach consists of a search for a maximum of the combined PDF, as described by Bosch (2004) for a similar problem. A sampling approach consists of producing a large set of joint model (reservoir-elastic properties) realizations in proportion to the combined probability. A sampling approach can provide a full description of the probability distributions and account for multiple modes in the solution, although this technique is more expensive computationally than the optimization approach.

Using Monte Carlo integration, probabilities can be calculated straightforwardly from the set of realizations of the probability density  $\sigma(\mathbf{m})$ , approximating the probability integral by a summation over the realizations normalized by their number. To explain two of the most common operations, let us consider a set of N realizations of the joint reservoir-elastic model  $\{\mathbf{m}^1, \mathbf{m}^2, \mathbf{m}^3, ..., \mathbf{m}^N\}$  and an arbitrary function  $h(\mathbf{m})$ , defined over the model space M. The expected value of the function  $h(\mathbf{m})$  for our true reservoir is shown in

$$E[h] = \int_{M} h(\mathbf{m})\sigma(\mathbf{m})d\mathbf{m} \approx \frac{1}{N} \sum_{n=1}^{N} h(\mathbf{m}^{n}).$$
 (9)

In particular, considering any volume of the model space A being a subset of the model parameter space and an indicator function  $I(\mathbf{m})$  that takes a value of one if  $\mathbf{m} \in A$  and 0 if  $\mathbf{m} \notin A$ , the probability of finding our true reservoir configuration within the volume A is as follows:

$$p(\mathbf{m} \in A) = E[I] = \int_{M} I(\mathbf{m}) \sigma(\mathbf{m}) d\mathbf{m} \approx \frac{1}{N} \sum_{n=1}^{N} I(\mathbf{m}^{n}).$$
(10)

Errors in the integral approximation tend to zero as the number of realizations N increases. Thus, model parameter probabilities and expected values can be estimated via simple computation of averages over the model realizations.

There is significant work in the discipline of statistics and related fields about algorithms to sample probability densities, and many techniques have been developed. For large parameter spaces and complex probability densities, most of these algorithms are based on Markov chains. The basic procedure is to start in an arbitrary configuration of model parameters, generating a chain of realizations by perturbing groups of model parameters iteratively. The way to modify the parameters follows statistical rules, which are applied at each iteration to warrant the convergence of the chain to a set of samples of the probability density. The choice of adequate and efficient sampling algorithms depends on the case, according to the dimensionality of the parameter space and the type of PDF, their conditionals, and factors.

In this work, we develop a sampling algorithm adapted to the relation between parameters and the specific structure of the combined probability density (in equation 4), combining several well-known sampling techniques: multivariate Gaussian, Gibbs, and metropolis samplers. We perform multivariate Gaussian simulations on subsets of model parameters, with basis on univariate Gaussian simulations of each parameter.

For this purpose, we use the common method of the product with a square root of the model covariance matrix,  $\mathbf{y} = \mathbf{C}^{1/2}\mathbf{x}$ , where  $\mathbf{x}$  are independent Gaussian deviates of unitary variance and  $\mathbf{y}$  are Gaussian deviates with covariance  $\mathbf{C}$ . We use the Gibbs sampler to expand marginal sampling of groups of parameters to all the parameter space. The Gibbs sampler is a technique for generating realizations of a multivariable probability by sampling from marginals of the probability over reduced subsets of the parameters, which are selected in sequence or randomly to cover the complete set of parameters.

In our method, we set up a Markov chain to sample from the prior probability densities over the reservoir properties  $\rho_{\rm geo}(\mathbf{m}_{\rm geo})$  and the seismic source parameters  $\rho_{\rm sou}(\mathbf{m}_{\rm sou})$  by multivariate Gaussian simulation from marginals of groups of parameters randomly selected at each step of the chain following a Gibbs sampling method. Sampling is extended to the physical parameter space by calculating the petrophysical transform of the reservoir parameter realization  $\mathbf{m}_{\rm geo}^{\rm n}$ , where n indicates the current step of the chain, and then adding Gaussian deviates of the appropriate covariance:

$$\mathbf{m}_{\text{phys}}^{\text{n}} = \mathbf{f}(\mathbf{m}_{\text{geo}}^{n}) + \mathbf{C}_{\text{phys}|\text{geo}}^{1/2} \mathbf{x}.$$
 (11)

Here, x are unitary variance independent Gaussian deviates. By repeating this procedure, we set up the chain convergent to the joint prior PDF over the model parameter space:

$$\rho(\mathbf{m}_{\text{phys}}, \mathbf{m}_{\text{geo}}, \mathbf{m}_{\text{sou}}) = \underbrace{\pi(\mathbf{m}_{\text{phys}} | \mathbf{m}_{\text{geo}})}_{\text{petrophysics}} \underbrace{\rho_{\text{geo}}(\mathbf{m}_{\text{geo}})}_{\text{geostatistics}} \underbrace{\rho_{\text{sou}}(\mathbf{m}_{\text{sou}})}_{\text{source}}.$$
(12)

We use the prior chain and the metropolis algorithm to produce a Markov chain convergent to the combined probability density (equation 4). Let us assume we have generated a realization  $\mathbf{m}^n = (\mathbf{m}_{phys}^n, \mathbf{m}_{geo}^n, \mathbf{m}_{sou}^n)$  in the current step of the chain n, with geophysical likelihood function  $L(\mathbf{m}^n) = L(\mathbf{m}_{phys}^n|\mathbf{m}_{sou}^n)$ , and want to produce the realization corresponding to the next step, n + 1. The metropolis sampler proceeds in the following way:

- Draw a candidate realization m<sup>cand</sup> with a step forward to the chain convergent to the joint prior probability density.
- Simulate the seismic data corresponding to this realization and calculate the geophysical likelihood function L(m<sup>cand</sup>).
- 3) Accept the candidate realization as next step of the chain,  $\mathbf{m}^{n+1} = \mathbf{m}^{\text{cand}}$ , with probability  $p = \min[1, (\mathbf{m}^{\text{cand}})/L(\mathbf{m}^n)]$ .

- If the candidate is rejected, repeat in the chain the current realization, m<sup>n+1</sup> = m<sup>n</sup>.
- 5) Go to operation 1 for the next step.

The chain generated in this way is convergent to the combined probability density (equation 4). Work by Hastings (1970), Geyer (1992), Tierney (1994), Smith and Roberts (1993), Mosegaard and Tarantola (1995), and Bosch (1999) are sources of additional information on the Markov-chain Monte Carlo sampling methods described.

### Geophysical, petrophysical, and geostatistical modeling

In this work, we consider the case of inverting short-offset seismic stacked and time-migrated data, which we simulate as zero-offset seismic data reflected in a horizontally layered medium. We parameterize the medium in time as a series of homogeneous horizontal layers described by acoustic impedance and total porosity. Time thickness of the layers is uniform and related with the seismic vertical resolution, approximately one-quarter of the dominant seismic period. With this setting, we independently invert each common-depthpoint (CDP) trace in the seismic volume, estimating a 1D model of acoustic impedance and total porosity per CDP location.

Our description of the reservoir is conditioned by the type of data. Because the stacked short-offset reflection data are influenced mostly by acoustic impedance, the latter is the natural choice for the physical property to include in the medium model. Conversely, acoustic impedance in clastic rocks commonly is influenced strongly by total porosity. Hence, we select this property to characterize the reservoir in our model. Other reservoir properties affect the acoustic impedance. We model the impedance with a deterministic component dependent of porosity and a random component that embodies the additional effects, which are statistically characterized from well-log data. Our method also would be valid for other reservoir properties strongly related to acoustic impedance and could be case dependent. A more complete description, including facies and fluids, could be considered, particularly for inverting prestacked seismic data, but it is beyond the scope of the current example.

The seismic data are simulated from a realization of the acoustic impedance by calculating the reflectivity series and convolving it with the source wavelet. This operation provides us with the geophysical forward function  $\mathbf{g}(\mathbf{m}_{phys},\mathbf{m}_{sou})$  considered in equation 7 of the geophysical likelihood function. This simulation method does not account for all phenomena involved in wave propagation and is clearly one-dimensional in the medium description for each CDP location. However, this type of simulation is used widely in inversion algorithms applied to reflection seismic data because of its simplicity and low computational cost.

In particular, for a Monte Carlo method, where a large number of repeated simulations are generated, the computational cost is a relevant issue in selecting the forward simulation algorithm. However, there is no limitation in the present formulation for considering a more elaborate seismic simulation method, such as finite differences or a reflectivity calculation in a 3D model. Finally, the data covariance matrix in this formulation,  $\mathbf{C}_{\text{dat}}$  in equation 7, characterizes the combined data uncertainty that represents the addition of observation, simulation, and modeling error variances.

For the relation between total porosity and acoustic impedance, we use a mixed model described in equation 11. We model the acoustic impedance as a random field conditioned by the total porosity field, with a central value that is a petrophysical transform of the po-

O34 Bosch et al.

rosity  $\mathbf{f}(\mathbf{m}_{geo})$  plus multivariate Gaussian deviations. Here, we use a relation directly derived from the Wyllie transform for the compressional velocity (Wyllie et al., 1956) and corresponding to density as the petrophysical transform of the porosity to acoustic impedance,

$$Z(\phi) = V_{\text{matrix}} \rho_{\text{matrix}} \frac{\left[1 - \phi \left(1 - \frac{\rho_{\text{fluid}}}{\rho_{\text{matrix}}}\right)\right]}{\left[1 - \phi \left(1 - \frac{V_{\text{matrix}}}{V_{\text{fluid}}}\right)\right]}, \quad (13)$$

with Z being the layer acoustic impedance,  $\phi$  the layer total porosity, and  $\rho_{\text{fluid}}$ ,  $\rho_{\text{matrix}}$ ,  $V_{\text{matrix}}$ , and  $V_{\text{fluid}}$  the mass density and compressional velocities for the pure rock matrix and pure fluid, respectively.

The total porosity, by definition, is a property bounded by zero and one and, as such, cannot be Gaussian distributed. For all statistical modeling, we use the logarithmic porosity, which is the logarithm of the pore and matrix volume ratio, instead of the porosity as the model property. The logarithmic porosity is defined conveniently in the complete real axis and can be modeled with Gaussian densities. Figure 3 shows Gaussian probability densities defined in the domain of

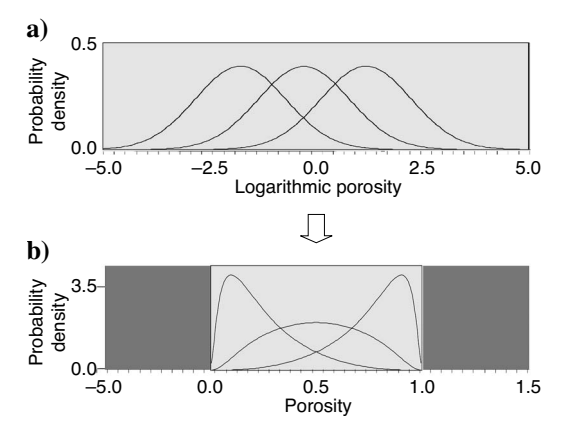


Figure 3. Gaussian probability densities in the logarithmic porosity domain and the corresponding densities in the porosity domain.

Table 2. Petrophysical parameters and statistics used in the synthetic test of the method.

Statistical parameter	Value
Logarithmic porosity prior mean	-1.735 (corresponding to 0.15 porosity)
Logarithmic porosity prior standard deviation	0.7
Logarithmic porosity covariance function	Spherical model with a range of 60 ms
Impedance standard deviation from transform	$10^6 \text{ kg s}^{-1} \text{ m}^{-2}$
Impedance deviation covariance function	Spherical model with a range of 60 ms
Wyllie transform parameter $V_{ m matrix}$	5600 m/s
Wyllie transform parameter $V_{ m fluid}$	1587 m/s
Wyllie transform parameter $ ho_{ ext{matrix}}$	$2600 \text{ kg/m}^3$
Wyllie transform parameter $ ho_{ m fluid}$	$1000 \text{ kg/m}^3$
Seismic data misfit standard deviation	5% of seismic amplitude range
Seismic data misfit covariance function	Time uncorrelated

the logarithmic porosity and the corresponding densities in the domain of the porosity. The resulting model for the probability in the porosity domain is similar to the lognormal near the zero bound, opposite lognormal close to the one bound and similar to the Gaussian at the middle of the range.

The transformation of the porosity to the logarithmic porosity  $\phi^*$  is given by  $\phi^* = \ln[\phi/(1-\phi)]$ , whereas the inverse transformation is  $\phi = \exp[\phi^*]/(1+\exp[\phi^*])$ . The impedance transform (relation 13) in terms of the logarithmic porosity is

$$Z(\phi^*) = V_{\text{matrix}} \rho_{\text{matrix}} \frac{\left(1 + \exp[\phi^*] \frac{\rho_{\text{fluid}}}{\rho_{\text{matrix}}}\right)}{\left(1 + \exp[\phi^*] \frac{V_{\text{matrix}}}{V_{\text{fluid}}}\right)}. \quad (14)$$

We calibrate the petrophysical transform to the reservoir data by adjusting the  $\rho_{\text{fluid}}$ ,  $\rho_{\text{matrix}}$ ,  $V_{\text{matrix}}$ , and  $V_{\text{fluid}}$  to optimal values that produce a best fit of the well-log data in the time window of interest. We assume these parameters of the petrophysical transform are uniform for this time window. This is an approximation because fluid and matrix elastic properties are variable with the reservoir stratification. The deviations from the relation, caused by local variations of fluids and matrix properties, are characterized statistically to obtain the covariance matrix  $\mathbf{C}_{\text{phys}|\text{geo}}$  in equations 8 and 11, needed for the mixed petrophysical model explained in the previous section. Thus, we account for porosity-variation effects in the deterministic component of our impedance model (the Wyllie transform) and for facies and fluid effects in the random component that characterizes deviations from the transform.

Concerning the geostatistical model of the logarithmic porosity, we calculate from the well-log data the mean logarithmic porosity in the window of interest and characterize the deviations from the mean to obtain the covariance matrix  $\mathbf{C}_{\text{geo}}$  used in equation 5.

## SYNTHETIC TEST

We tested our sampling algorithms with a numerical model. In this case, we did not use a specific data set to calibrate the porosity-im-

pedance relation or characterize the property statistics. Table 2 shows statistical and petrophysical parameters that we used to build a joint porosity-impedance realization taken as the true medium for this example. The covariance functions described are one dimensional, as are the porosity and impedance models. The seismic trace computed by convolving a source function with the reflectivity series obtained from the true impedance profile was taken as the observed data. We ran the sampling algorithm described in the previous section, producing a large chain of joint porosity-impedance realizations, starting from a model configuration corresponding to a uniform mean prior porosity and acoustic impedance.

Figure 4 shows a curve of data residuals versus the iterations of the Monte Carlo method, plotted for two different iteration ranges. Each iteration involves testing a perturbation of the porosity or impedance applied in a subset of layers taken randomly and recalculating the seismic trace. The vertical axis indicates the chi-squared statistic of

the residuals. This is computed by the sum of squared differences between calculated and observed seismic amplitudes divided by the data variance and the number of data samples. The horizontal axis indicates the number of steps in the Markov chain, each one associated with an accepted or rejected perturbation of the porosity-impedance model configuration.

The first phase of the chain, associated with the starting configuration and large residuals, is called the burn-in phase. Once residuals are reduced, the joint porosity-impedance model realizations satisfactorily explain the seismic data within the data errors. This is called the sampling phase. Realizations produced during the sampling phase are considered samples from the combined probability density. Figure 4 also shows a curve indicating the progress of the joint data and model residuals, calculated by adding the corresponding chi-squared statistics for the seismic data residuals, the impedance deviations from the Wyllie transform of the porosity, the porosity deviations from the prior porosity, and the source wavelet deviation from the prior estimate.

The model configurations were modified during the sampling phase, but they remain within the geophysical and petrophysical likelihoods, as shown in Figures 5 and 6. Figure 5 shows eight realizations taken at regular intervals in the sampling phase of the chain,

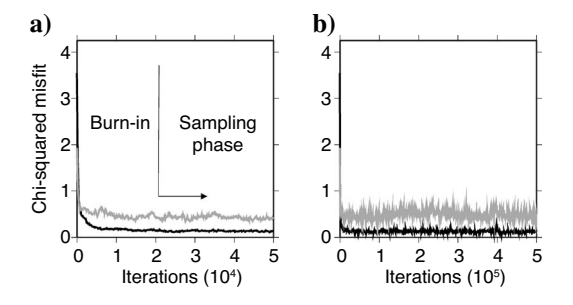


Figure 4. Progress with the iterations in the sampling algorithm of the chi-squared seismic amplitude residual (black line) and the chi-squared joint data and model residuals (gray line): (a) 50,000 iterations; (b) 500,000 iterations.

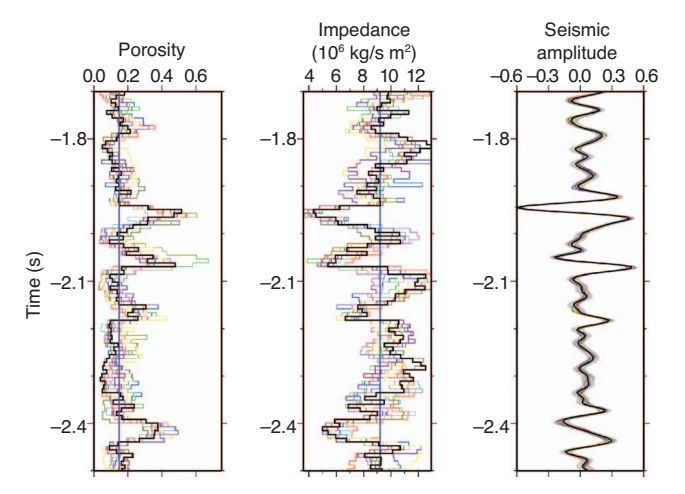


Figure 5. Eight joint porosity-impedance realizations taken at regular intervals from the sampling chain and their corresponding calculated seismic data (various color lines). Superimposed are the true model configuration and the observed data (black lines). The gray band shows one standard deviation of data uncertainty centered in the observed data. Initial model configurations for porosity and impedance are shown with a straight blue line.

all fitting the seismic observed data within data uncertainties. They indicate the features and variability of the total porosity and the acoustic impedance. Figure 6 shows the porosity and impedance crossplot for the same realizations shown in Figure 5. The solid line indicates the petrophysical transform (i.e., Wyllie relation), with parameters indicated in Table 2, and the gray area plus or minus one standard deviation for deviates from the relation. This figure illustrates that joint porosity-impedance realizations also honor the petrophysical information prescribed in the petrophysical likelihood function.

We obtained 480,000 realizations from the sampling phase of the chain. From this set of realizations, we computed the expected value of the porosity and impedance and the marginal probabilities for the porosity and impedance as a function of two-way reflection time. These computations are straightforward averages of model realizations within the sampling phase, as described by equations 9 and 10. Figure 7 shows the cumulative marginal probability distribution for

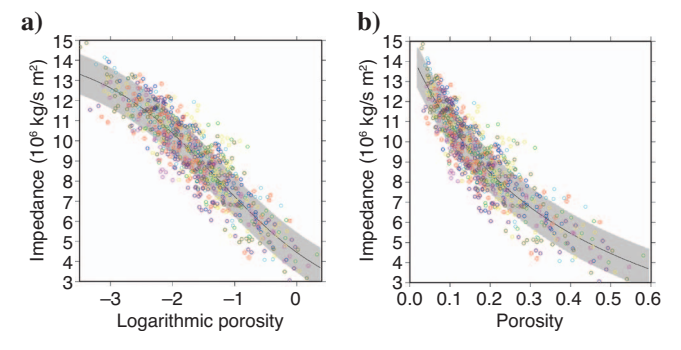


Figure 6. Layer acoustic impedance and total porosity (color circles) for the eight realizations shown in Figure 7, displayed with a horizontal axis corresponding to (a) the logarithmic porosity and (b) the porosity. The gray band shows one standard deviation of the logarithmic porosity in the statistical model that links the two properties, centered at the Wyllie petrophysical transform (black line).

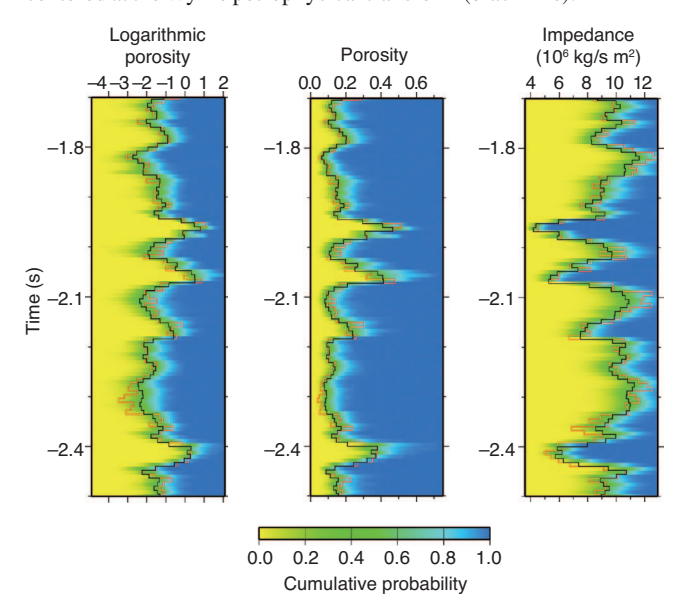


Figure 7. Total porosity and acoustic impedance estimated with the inversion (black line), corresponding to the true model (red line) used in the synthetic test. The color image shows the cumulative probability density for porosity and impedance at each time obtained as a result of the inversion.

O36 Bosch et al.

the porosity and the impedance, the porosity and impedance estimated by the inversion, and the true porosity and impedance profiles. The figure shows adequate prediction of the true values for the synthetic test, with identification of major stratification depicted by low and high porosity and corresponding high and low impedance. The correlation between estimated and true properties was 0.91 for the acoustic impedance and 0.87 for the total porosity.

For comparison with these results, we made the calculations using the same Monte Carlo sampling techniques adapted to the corresponding formulation in separate estimation steps: (1) inverting the seismic data to estimate the acoustic impedance (with independence from the porosity) and (2) transforming the estimated impedance to porosity with the inverse Wyllie relation. Table 3 compares the joint and separate inversions based on the correlation between the estimated and true porosity and impedance and the rms estimation error. The results of the joint inversion are correlated better with the true porosity and impedance. In addition, the rms estimation error is smaller for the joint inversion results than for those corresponding to the separate inversion — approximately 8% smaller for the impedance and 23% smaller for the porosity. From a mathematical point of view, the joint inversion can be decoupled in two separate steps only in the case of a linear petrophysical transform (Bosch, 2004). The referred work shows additional synthetic examples comparing joint and separate inversions, solved with an optimization method.

# APPLICATION TO SEISMIC AND WELL-LOG RESERVOIR DATA

We applied our method to a data set from an eastern Venezuelan oil reservoir. This reservoir is in a formation of clastic rocks characterized by sequences of sand and shale. Fluids filling the pores are brine and oil; no gas is present. First, we upscaled the acoustic impedance and total porosity profiles derived from well-log data to the corresponding seismic scale (Figure 8). Appropriate upscaling for the total porosity is the arithmetic average of the small layers' total porosities. The impedance does not upscale in the same way; we used a relation that results from the combination of the Backus average for the compressional velocity and the arithmetic average for the mass density. Using a regression method, we adjusted Wyllie transform parameters  $\rho_{\rm fluid}$ ,  $\rho_{\rm matrix}$ ,  $V_{\rm matrix}$ , and  $V_{\rm fluid}$  in the time window of interest to fit the actual upscaled well data. Figure 9 shows the total porosity and acoustic impedance crossplot derived from the well-log data, superimposed on the Wyllie transform calibrated to fit the data.

Table 3. Prediction rms error and correlation factor between predicted and true property values obtained with the joint and two-step inversion approaches.

Description	Joint inversion	Two-step inversion
Predicted true porosity correlation	0.87	0.82
Predicted true logarithmic porosity correlation	0.84	0.78
Predicted true impedance correlation	0.91	0.89
Porosity prediction root mean square error	0.043	0.053
Logarithmic porosity prediction rms error	0.33	0.43
Impedance prediction rms error (kg/m $s^2$ )	$0.85 \times 10^{6}$	$0.92 \times 10^{6}$

In the well-log data, we also characterized the deviations of the acoustic impedance from the corresponding values predicted by the Wyllie transform of the porosity by calculating the deviation covariance for different time lags and modeling the covariance function. Figure 10a shows the covariance function for the deviations of the acoustic impedance from the petrophysical transform (i.e., the calibrated Wyllie transform) and the modeled covariance function. To model the covariance function, we used a mixed model: the addition of a nugget term, a Gaussian term, and an exponential term, with parameters fitted to the covariance data. With this model, we defined the covariance matrix  $\mathbf{C}_{\text{phys}|\text{geo}}$  in equations 8 and 11. By characterizing the petrophysical transform deviation covariance and applying corresponding deviations in the statistical petrophysical modeling, we accounted for the impedance variability associated with factors

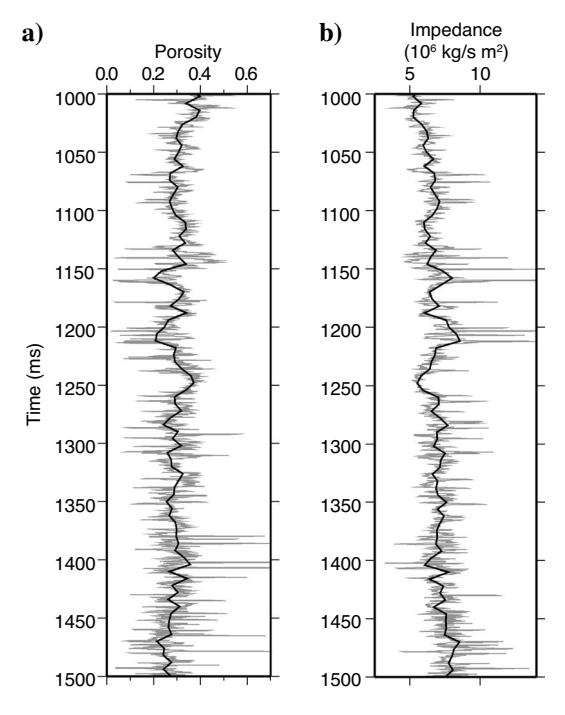


Figure 8. (a) Total porosity and (b) acoustic impedance plots obtained from the well-logged data (gray line) and the corresponding profile upscaled to a 6-ms sampling after appropriate averaging of thin layer values (black line).

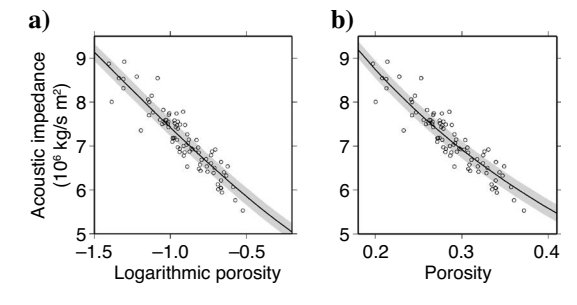


Figure 9. Crossplot of acoustic impedance and total porosity obtained from the well-logged data after scaling to the model sampling interval of 6 ms (black circles), the Wyllie transform with parameters obtained by regression to fit the data (black line), and the one standard deviation band that characterizes impedance deviations from the predicted Wyllie transform value (gray band). Impedance data are plotted against (a) the logarithmic porosity and (b) the porosity.

that affect the impedance in addition to the porosity, such as variations in fluids and lithology.

Similarly, we characterized the logarithmic porosity obtained from the well-logged data by estimating the mean logarithmic porosity and the covariance function. The covariance for different time lags and the modeled covariance function are shown in Figure 10b. We used the modeled covariance function to define the prior covariance matrix for the porosity  $\mathbf{C}_{\text{geo}}$  and the mean logarithmic porosity to define the prior expected porosity profile  $\mathbf{m}_{\text{geo prior}}$  in equation 5. In this case, we used a mixed model to fit the covariance data, adding a nugget term, an exponential term, and a damped cosine term. The latter was appropriate to model the oscillating component of the covariance that results from the stratified nature of the porosity profile, driven by the shale-sand sequences.

We used the common least-squares method described by Oldenburg et al. (1991) to estimate a source wavelet at the location of the available well data. This method combines the impedances calculated from the well-log data with the measured seismic data at the well location. The source wavelet is parameterized by the amplitude sampled at regular time intervals, corresponding to the same sampling interval of the seismic data. The resulting wavelet is taken as the center of the prior probability density for the wavelet information  $\mathbf{m}_{\text{sou prior}}$  in equation 6. We allowed variability of the model source wavelet to adapt to spatial changes, with a standard deviation from the estimated wavelet of 20% of the total amplitude range of the wavelet

We applied the inversion method described to generate 1 million joint porosity-impedance realizations, fully exploring the solution space. To obtain a volume of the estimated properties, we applied this procedure in a trace-by-trace manner to a seismic cube in the area. Figure 11 shows the estimated total porosity and acoustic impedance for a section of this seismic cube. The estimated values were calculated by the average values of the realizations in the sampling phase. The acoustic impedances and porosities derived from the well data were superimposed at the well location for comparison with the predicted porosity and impedance fields. In addition, we superimposed the observed seismic data all through the section for comparison with the estimated property fields.

In Figure 11, we can highlight the coherence between the stratification in the estimated porosity and impedance fields and the corresponding observed seismic refection events. Vertical resolution in the estimated fields reaches, in some section locations, the maximum section in the estimated fields reaches.

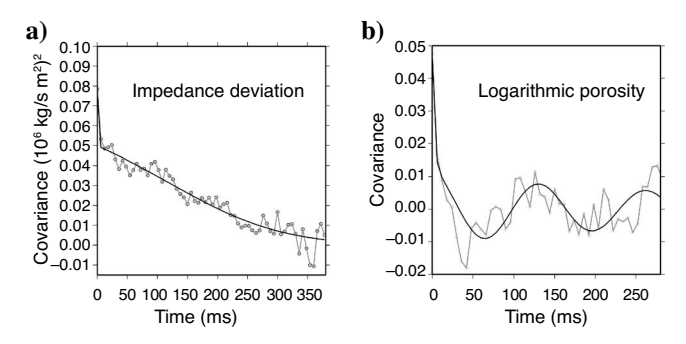


Figure 10. Time covariance for (a) deviations of the well-logged impedance from the Wyllie transform of the well-logged porosity and (b) the total porosity. The covariance calculated from the well-logged data is shown in black circles joined by gray line segments; the corresponding covariance function model fitted to the data is shown with a black line.

mum expected model resolution of 6 ms, approximately one-quarter of the dominant period of the seismic signal, showing a thin stratum that can be followed across the traces. In addition, the figure shows adequate correlation between the strata of high and low porosities and impedances, estimated by the seismic inversion and the corresponding estimate at the well location from the wire logs. A normal fault present in this reservoir, with a vertical displacement of approximately 20 ms, is also shown in the figure, with a corresponding displacement that can be identified in the property fields.

As explained, the model parameters included the source wavelet, which is jointly estimated by the Monte Carlo inversion method. Figure 12 shows the prior estimated source wavelet and ten realizations of the source wavelet taken at regular intervals from the sampling chain at the location of the well. This realization shows a slight correction from the prior estimated wavelet. Posterior probabilities for the source wavelet amplitudes are shown in the same figure, as is the posterior best estimate, which is calculated by the average of the sampled wavelet realizations.

A summary of the information obtained from our Monte Carlo inversion at the well is shown in Figure 13. The figure shows a cumulative marginal probability plot for the porosity and impedance calculated from the total sampled realizations. The posterior expected values of the total porosity and acoustic impedance are superimposed onto the probability plot. These are calculated by averaging the total porosity and acoustic impedance realizations in the sampling phase of the chain. The total porosity and acoustic impedance calculated from the well-log data also are plotted. The basic stratification can be identified by zones of low and high porosity, corresponding to zones of high and low impedance, in both the probability plots and the estimated time profiles. The same sequences are indicated by porosity and impedance calculated from the well-log data. Well-log-derived and seismic-derived values show a significant correlation of 0.7 for the acoustic impedance and 0.69 for the total porosity.

Figure 13 shows the observed seismic data and a one standard deviation of the data uncertainty bar prescribed for the inversion,

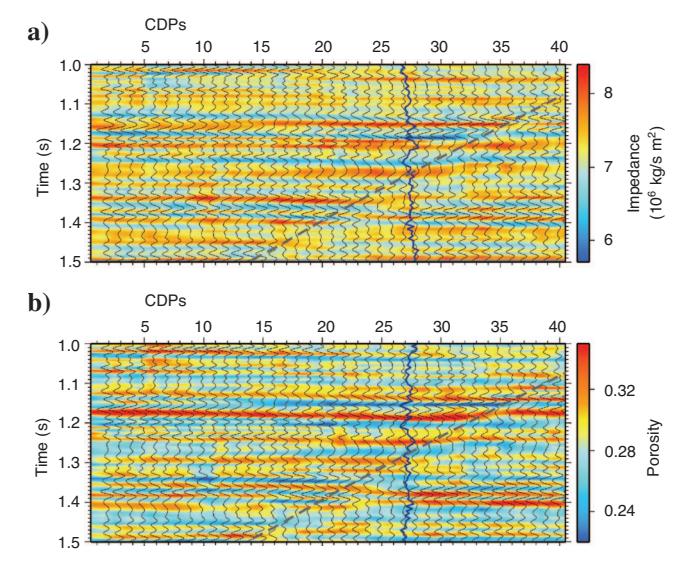


Figure 11. Sections of the (a) acoustic impedance and (b) total porosity estimated with the inversion, superimposed onto the corresponding well-logged property (thick blue line) and the observed seismic data (thin black lines). The trace of a normal fault that intercepts the section is shown (dashed gray line).

O38 Bosch et al.

which corresponds to the 15% of the observed seismic data amplitude range. The calculated data from a realization taken at random are also shown. All joint model realizations explain the seismic data within data uncertainties and also honor the petrophysical transform within the prescribed deviations.

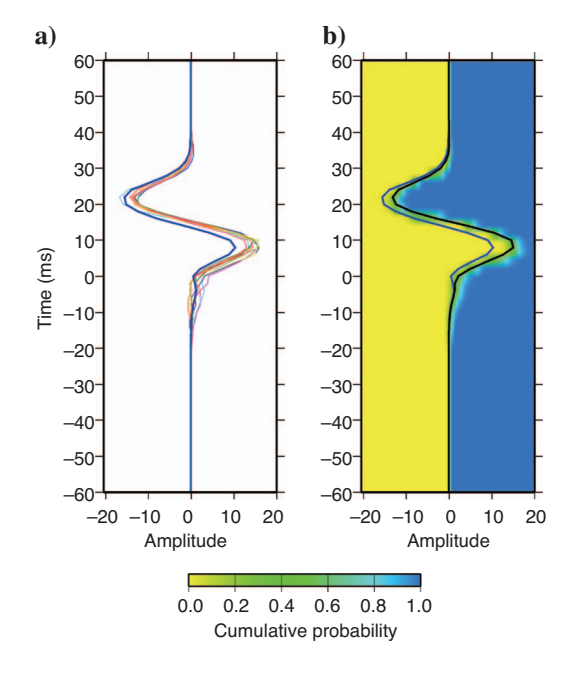


Figure 12. (a) Prior seismic source (thick dark blue line) and 10 seismic source realizations pulled at regular intervals from the sampling phase at the well location (various colored lines). (b) Cumulative probability plot for the seismic source, the prior seismic source (blue line), and the average of realizations in the sampling phase (black line).

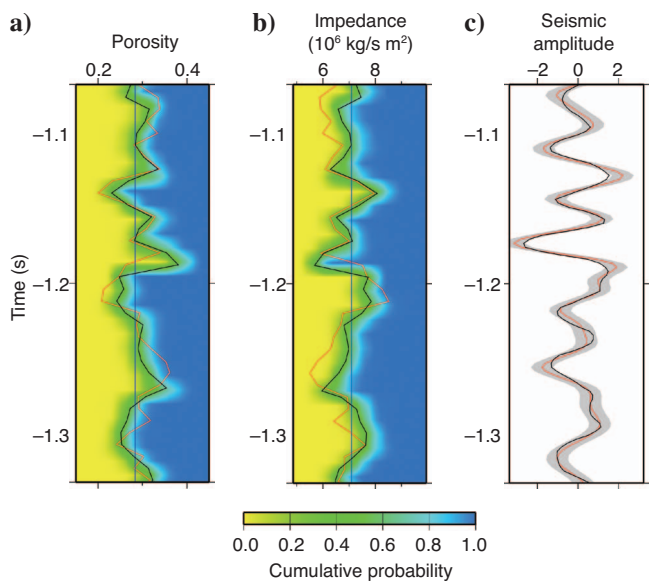


Figure 13. (a) Porosity and (b) impedance cumulative probability plots with the mean porosity and impedance profiles obtained as a result of the inversion (black lines) and the porosity and impedance profiles obtained from the well-logged data (red lines). (c) One-standard-deviation data uncertainty band is centered at the observed seismic data (red line), and seismic data are calculated from a model realization taken at random (black line).

#### DISCUSSION

We describe a general methodology for the estimation of reservoir parameters from seismic amplitudes, which we implement in a field case assuming: (1) a one dimensional reservoir model per stacked trace, (2) the simulation of the seismic data by convolving a source wavelet with the reflectivity series calculated from the model, and (3) a strong relation between the total porosity and the acoustic impedance in the area. The latter is a condition that we confirm with our well-log data. However, the general formulation we propose is not restricted by these assumptions. More complete seismic simulation techniques or petrophysical models could be used within a similar framework.

Our choice of reservoir properties in the joint model exploits the relation between the total porosity and the acoustic impedance, which is described by the Wyllie transform. This relation is valid for a wide range of rocks, including clastic environments as the one we considered. In addition to the porosity, the Wyllie transform depends on parameters that characterize the elastic behavior of the matrix and the fluid filling the pores, which are variable within the reservoir. We use uniform elastic parameters for the transform, optimized to the best fit of the well data within the time window of interest. Thus, factors such as fluid and facies variations produce deviations from the transform that are accounted in the random component of our petrophysical model. The deviations and their time covariance are characterized from the well-log data and included in the model. Our mixed petrophysical model (deterministic mean plus random deviates) does not assume an exact relation between the porosity and the impedance, and statistically honors the dispersion from the Wyllie transform.

Other reservoir properties related with the acoustic impedance could be used in the joint reservoir description. Although it was out of the scope of the present example, a more complete petrophysical model could be considered, including facies and fluid parameters as reservoir properties. It would depend on the specific case whether a set of reservoir parameters may be resolved by the seismic and petrophysical information. A natural extension of the method would be the inversion of prestacked seismic data to estimate elastic parameters and additional reservoir properties. Similarly, another promissory line of development consists of including well log conditioning to the model, which could increase vertical resolution close to the wells and warrant the model to honor the well data at well locations.

# CONCLUSIONS

We integrate, under a unified petrophysical and geophysical inversion scheme, different types of information and data that contribute to the estimation of reservoir and elastic parameters. Specifically, we invert poststacked short offset seismic data to infer the total porosity and the acoustic impedance fields, honoring petrophysical relations calibrated to crossplots of well-log data. The joint formulation helps to appropriately combine different uncertainties into the final reservoir field estimate: seismic data uncertainty, data deviations from the petrophysical transform, and seismic source uncertainty. The joint inversion method fully accounts for nonlinear relations between the seismic data, elastic parameters, and reservoir parameters.

Our formulation is made in a probabilistic inference framework and the solution consists in sampling realizations from the posterior probability density, which results from the combination of geophysical, petrophysical, and prior reservoir information. Hence, the porosity-impedance realizations jointly honor the complete set of information. We compute from the realizations, expected values and complete descriptions of the marginal probability for the reservoir and elastic properties in the model. Although components of the posterior probability are modeled with Gaussian functions, they are evaluated at nonlinear functions of the model parameters and the resulting posterior probability is not Gaussian. The sampling method approach is general enough to account for non-Gaussian, complex, eventually multimodal, posterior probability densities.

A synthetic test of the method showed very good correlation between predicted and true model values, both for porosity and impedance. In this example, we illustrate that the joint inversion produces a better prediction of the reservoir and elastic field than the step-wise inversion. The application to a field case also showed good correlation between the porosity and impedance values estimated with the inversion and the corresponding values estimated from well-log data. Although we used the well-log derived properties to calibrate the petrophysical relationship between the porosity and the acoustic impedance, the actual information of the well derived properties, as a time profile, was not used to condition the estimation. Thus, the well data derived acoustic impedance and total porosity time profiles remain a valid reference for comparison of the inversion results. The present method provides a full description of the result uncertainty, as illustrated by the marginal probability plots for the porosity and impedance. These model uncertainties account for the combination of uncertainties corresponding to the geophysical and petrophysical components of the inference problem.

#### ACKNOWLEDGMENTS

We acknowledge Petrobras Energía Venezuela, the Universidad Central de Venezuela, and the CDCH-UCV (PG-08-00-5631-2004 and PI-08-00-5627-2004) for support in this research. We thank referees and GEOPHYSICS editors K. Wapenaar and M. D. Sacchi for their reviews.

## REFERENCES

Bachrach, R., 2006, Joint estimation of porosity and saturation using stochastic rock-physics modeling: Geophysics, 71, no. 5, O53-O63.

Bosch, M., 1999, Lithologic tomography: From plural geophysical data to lithology estimation: Journal of Geophysical Research, 104, 749–766.

——, 2004, The optimization approach to lithological tomography: Com-

- bining seismic data and petrophysical information for porosity prediction: Geophysics, **69**, 1272–1282.
- Bosch, M., L. Cara, and A. Navarro, 2006, Joint estimation of reservoir and elastic parameters from seismic amplitudes using a Monte Carlo method: 76th Annual International Meeting, SEG, Expanded Abstracts, 2027– 2031.
- Bosch, M., and E. Fernández, 2003, Porosity probability calculation from lithological inversion of seismic amplitudes: Presented at the 2003 Summer Research Workshop, SEG.
- Bosch, M., A. Guillen, and P. Ledru, 2001, Lithologic tomography: An application to geophysical data from the Cadomian belt of northern Brittany, France: Tectonophysics, **331**, 197–227.
- Bosch, M., and J. McGaughey, 2001, Joint inversion of gravity and magnetic data under lithological constraints: The Leading Edge, 20, 877–881.
- Contreras, A., C. Torres-Verdin, W. Chesters, and K. Kvien, 2005, Joint stochastic inversion of petrophysical logs and 3D pre-stack seismic data to assess the spatial continuity of fluid units away from wells: Application to a Gulf-of-Mexico deepwater hydrocarbon reservoir: Transactions of the 46th Annual Logging Symposium, Society of Petrophysicists and Well Log Analysts. 1–15.
- Doyen, P. M., 1988, Porosity from seismic data: A geostatistical approach: Geophysics, **53**, 1263–1275.
- Eidsvik, J., P. Avseth, H. Omre, T. Mukerji, and G. Mavko, 2004, Stochastic reservoir characterization using prestack seismic data: Geophysics, 69, 978–993.
- Geyer, C. J., 1992, Practical Markov chain Monte Carlo: Statistical Science, 7, 473–551.
- González, E. F., G. Mavko, and T. Mukerji, 2006, Rock physics and multiplepoint geostatistics for seismic inversion: 76th Annual International Meeting, SEG, Expanded Abstracts, 2047–2051.
- Hastings, W. K., 1970, Monte Carlo sampling method using Markov chains and their applications: Biometrika, **57**, 97–109.
- Larsen, A. L., M. Ulvmoen, H. Omre, and A. Buland, 2006, Bayesian lithology/fluid prediction and simulation on the basis of a Markov-chain prior model: Geophysics, 71, no. 5, R69–R78.
- Loures, L. G. L., and F. S. Moraes, 2006, Porosity inference and classification of siliciclastic rocks from multiple data sets: Geophysics, 71, no. 5, O65–O76
- Mosegaard, K., and A. Tarantola, 1995, Monte Carlo sampling of solutions to inverse problems: Journal of Geophysical Research, **100**, 12431–12447.
- Mukerji, T., A. Jørstad, P. Avseth, G. Mavko, and J. R. Granli, 2001, Mapping lithofacies and pore-fluid probabilities in a North Sea reservoir: Seismic inversions and statistical rock physics: Geophysics, 66, 988–1001.
- Oldenburg, D. W., S. Levy, and K. P. Whittall, 1991, Wavelet estimation and deconvolution: Geophysics, 46, 1528–1542.
- Smith, A. F., and G. O. Roberts, 1993, Bayesian computations via the Gibbs sampler and related Markov chain Monte Carlo methods: Journal of the Royal Statistical Society, 55, 3–23.
- Tarantola, A., 2005, Inverse problem theory and methods for model parameter estimation: SIAM.
- Tierney, L., 1994, Markov-chains for exploring posterior distributions: Annals of Statistics, 22, 1702–1762.
- Torres-Verdin, C., M. Victoria, G. Merletti, and J. Pendrel, 1999, Trace-based and geostatistical inversion of 3-D seismic data for thin-sand delineation: An application in San Jorge basin, Argentina: The Leading Edge, 19, 1070–1077.
- Wyllie, M. R. J., A. R. Gregory, and L. W. Gardner, 1956, Elastic wave velocities in heterogeneous and porous media: Geophysics, 21, 41–70.